2

Analysis of Composite Materials

2.1 Constitutive Relations

Laminated composites are typically constructed from orthotropic plies (laminae) containing unidirectional fibers or woven fabric. Generally, in a macroscopic sense, the lamina is assumed to behave as a homogeneous orthotropic material. The constitutive relation for a linear elastic orthotropic material in the material coordinate system (Figure 2.1) is [1–6]

$$\begin{bmatrix} \varepsilon_1 \\ \varepsilon_2 \\ \varepsilon_3 \\ \gamma_{23} \\ \gamma_{13} \\ \gamma_{12} \end{bmatrix} = \begin{bmatrix} S_{11} & S_{12} & S_{13} & 0 & 0 & 0 \\ S_{12} & S_{22} & S_{23} & 0 & 0 & 0 \\ S_{13} & S_{23} & S_{33} & 0 & 0 & 0 \\ 0 & 0 & 0 & S_{44} & 0 & 0 \\ 0 & 0 & 0 & 0 & S_{55} & 0 \\ 0 & 0 & 0 & 0 & 0 & S_{66} \end{bmatrix} \begin{bmatrix} \sigma_1 \\ \sigma_2 \\ \sigma_3 \\ \tau_{23} \\ \tau_{13} \\ \tau_{12} \end{bmatrix} \tag{2.1}$$

where the stress components (σ_i, τ_{ij}) are defined in Figure 2.1 and the S_{ij} are elements of the compliance matrix. The engineering strain components (ε_i, γ_{ij}) are defined as implied in Figure 2.2.

In a thin lamina, a state of plane stress is commonly assumed by setting

$$\sigma_3 = \tau_{23} = \tau_{13} = 0 \tag{2.2}$$

For Equation (2.1) this assumption leads to

$$\varepsilon_3 = S_{13}\sigma_1 + S_{23}\sigma_2 \tag{2.3a}$$

$$\gamma_{23} = \gamma_{13} = 0 \tag{2.3b}$$

Thus, for plane stress the through-the-thickness strain ε_3 is not an independent quantity and does not need to be included in the constitutive relationship. Equation (2.1) becomes

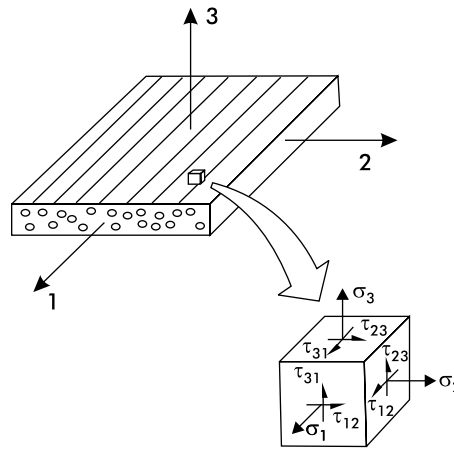

FIGURE 2.1
Definitions of principal material directions for an orthotropic lamina and stress components.

$$\begin{bmatrix} \varepsilon_1 \\ \varepsilon_2 \\ \gamma_{12} \end{bmatrix} = \begin{bmatrix} S_{11} & S_{12} & 0 \\ S_{12} & S_{22} & 0 \\ 0 & 0 & S_{66} \end{bmatrix} \begin{bmatrix} \sigma_1 \\ \sigma_2 \\ \tau_{12} \end{bmatrix} \tag{2.4}$$

The compliance elements S_{ij} may be related to the engineering constants (E_1, E_2, G_{12}, ν_{12}, ν_{21}),

$$S_{11} = 1/E_1, \quad S_{12} = -\nu_{12}/E_1 = -\nu_{21}/E_2 \tag{2.5a}$$

$$S_{22} = 1/E_2, \quad S_{66} = 1/G_{12} \tag{2.5b}$$

The engineering constants are average properties of the composite ply. The quantities E_1 and ν_{12} are the Young's modulus and Poisson's ratio, respectively, corresponding to stress σ_1 (Figure 2.2a)

$$E_1 = \sigma_1/\varepsilon_1 \tag{2.6a}$$

$$\nu_{12} = -\varepsilon_2/\varepsilon_1 \tag{2.6b}$$

E_2 and ν_{21} correspond to stress σ_2 (Figure 2.2b)

$$E_2 = \sigma_2/\varepsilon_2 \tag{2.7a}$$

$$\nu_{21} = -\varepsilon_1/\varepsilon_2 \tag{2.7b}$$

For a unidirectional composite E_2 is much less than E_1, and ν_{21} is much less than ν_{12}. For a balanced fabric composite $E_1 \approx E_2$ and $\nu_{12} \approx \nu_{21}$. The Poisson's ratios ν_{12} and ν_{21} are not independent

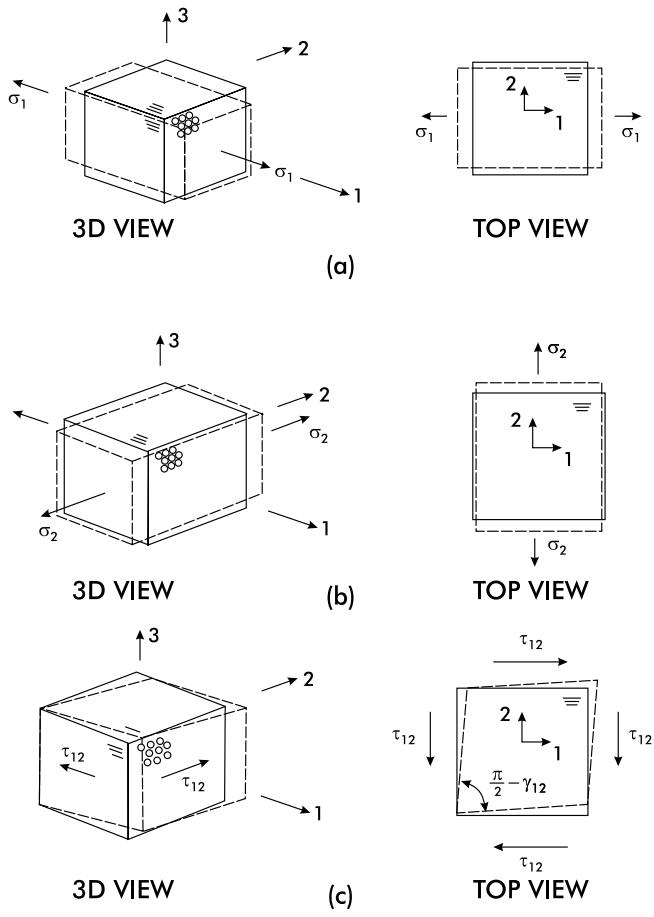

FIGURE 2.2
Illustration of deformations of an orthotropic material due to (a) stress σ_1, (b) stress σ_2, and (c) stress τ_{12}.

$$\nu_{21} = \nu_{12}E_2/E_1 \tag{2.8}$$

The in-plane shear modulus, G_{12}, is defined as (Figure 2.2c)

$$G_{12} = \tau_{12}/\gamma_{12} \tag{2.9}$$

It is often convenient to express stresses as functions of strains. This is accomplished by inversion of Equation (2.4)

$$\begin{bmatrix} \sigma_1 \\ \sigma_2 \\ \tau_{12} \end{bmatrix} = \begin{bmatrix} Q_{11} & Q_{12} & 0 \\ Q_{12} & Q_{22} & 0 \\ 0 & 0 & Q_{66} \end{bmatrix} \begin{bmatrix} \varepsilon_1 \\ \varepsilon_2 \\ \gamma_{12} \end{bmatrix} \tag{2.10}$$

where the reduced stiffnesses, Q_{ij}, can be expressed in terms of the engineering constants

$$Q_{11} = E_1/(1 - \nu_{12}\nu_{21}) \tag{2.11a}$$

$$Q_{12} = \nu_{12}E_2/(1 - \nu_{12}\nu_{21}) = \nu_{21}E_1/(1 - \nu_{12}\nu_{21}) \tag{2.11b}$$

$$Q_{22} = E_2/(1 - \nu_{12}\nu_{21}) \tag{2.11c}$$

$$Q_{66} = G_{12} \tag{2.11d}$$

2.1.1 Transformation of Stresses and Strains

For a lamina whose principal material axes (1,2) are oriented at an angle, θ, with respect to the x,y coordinate system (Figure 2.3), the stresses and strains can be transformed. It may be shown [1–6] that both the stresses and strains transform according to

$$\begin{bmatrix} \sigma_1 \\ \sigma_2 \\ \tau_{12} \end{bmatrix} = [T] \begin{bmatrix} \sigma_x \\ \sigma_y \\ \tau_{xy} \end{bmatrix} \tag{2.12}$$

and

$$\begin{bmatrix} \varepsilon_1 \\ \varepsilon_2 \\ \gamma_{12}/2 \end{bmatrix} = [T] \begin{bmatrix} \varepsilon_x \\ \varepsilon_y \\ \gamma_{xy}/2 \end{bmatrix} \tag{2.13}$$

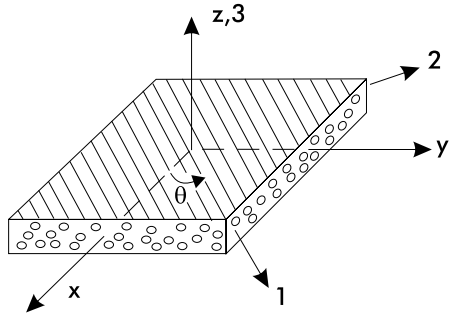

FIGURE 2.3
Positive (counterclockwise) rotation of principal material axes (1,2) from arbitrary x,y axes.

where the transformation matrix is [1–6]

$$[T] = \begin{bmatrix} m^2 & n^2 & 2mn \\ n^2 & m^2 & -2mn \\ -mn & mn & m^2 - n^2 \end{bmatrix} \tag{2.14}$$

and

$$m = \cos\theta \tag{2.15a}$$

$$n = \sin\theta \tag{2.15b}$$

From Equations (2.12) and (2.13) it is possible to establish the lamina strain–stress relations in the (x,y) coordinate system [1–6]

$$\begin{bmatrix} \varepsilon_x \\ \varepsilon_y \\ \gamma_{xy} \end{bmatrix} = \begin{bmatrix} \bar{S}_{11} & \bar{S}_{12} & \bar{S}_{16} \\ \bar{S}_{12} & \bar{S}_{22} & \bar{S}_{26} \\ \bar{S}_{16} & \bar{S}_{26} & \bar{S}_{66} \end{bmatrix} \begin{bmatrix} \sigma_x \\ \sigma_y \\ \tau_{xy} \end{bmatrix} \tag{2.16}$$

The $\bar{S}_{ij}$ terms are the transformed compliances defined in Appendix A. Similarly, the lamina stress–strain relations become

$$\begin{bmatrix} \sigma_x \\ \sigma_y \\ \tau_{xy} \end{bmatrix} = \begin{bmatrix} \bar{Q}_{11} & \bar{Q}_{12} & \bar{Q}_{16} \\ \bar{Q}_{12} & \bar{Q}_{22} & \bar{Q}_{26} \\ \bar{Q}_{16} & \bar{Q}_{26} & \bar{Q}_{66} \end{bmatrix} \begin{bmatrix} \varepsilon_x \\ \varepsilon_y \\ \gamma_{xy} \end{bmatrix} \tag{2.17}$$

where the overbars denote transformed reduced stiffness elements, defined in Appendix A.

2.1.2 Hygrothermal Strains

If fibrous composite materials are processed at elevated temperatures, thermal strains are introduced during cooling to room temperature, leading to residual stresses and dimensional changes. Figure 2.4 illustrates dimensional changes of a composite subjected to a temperature increase of ΔT from the reference temperature T. Furthermore, polymer matrices are commonly hygroscopic, and absorbing moisture leads to swelling of the material. The analysis of moisture expansion strains in composites is mathematically

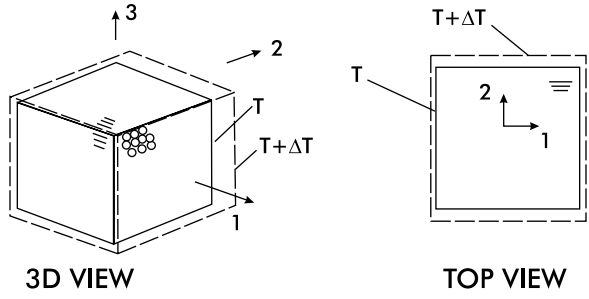

FIGURE 2.4
Deformation of a lamina subject to temperature increase.

equivalent to that for thermal strains [7,8] (neglecting possible pressure dependence of moisture absorption).

The constitutive relationship, when it includes mechanical-, thermal-, and moisture-induced strains, takes the following form [1,4]

$$\begin{bmatrix} \varepsilon_1 \\ \varepsilon_2 \\ \gamma_{12} \end{bmatrix} = \begin{bmatrix} S_{11} & S_{12} & 0 \\ S_{12} & S_{22} & 0 \\ 0 & 0 & S_{66} \end{bmatrix} \begin{bmatrix} \sigma_1 \\ \sigma_2 \\ \tau_{12} \end{bmatrix} + \begin{bmatrix} \varepsilon_1^T \\ \varepsilon_2^T \\ 0 \end{bmatrix} + \begin{bmatrix} \varepsilon_1^M \\ \varepsilon_2^M \\ 0 \end{bmatrix} \tag{2.18}$$

where superscripts T and M denote temperature- and moisture-induced strains, respectively. Note that shear strains are not induced in the principal material system by a temperature or moisture content change (Figure 2.4). Equation (2.18) is based on the superposition of mechanical-, thermal-, and moisture-induced strains. Inversion of Equation (2.18) gives

$$\begin{bmatrix} \sigma_1 \\ \sigma_2 \\ \tau_{12} \end{bmatrix} = \begin{bmatrix} Q_{11} & Q_{12} & 0 \\ Q_{11} & Q_{12} & 0 \\ 0 & 0 & Q_{66} \end{bmatrix} \begin{bmatrix} \varepsilon_1 & -\varepsilon_1^T & -\varepsilon_1^M \\ \varepsilon_2 & -\varepsilon_2^T & -\varepsilon_2^M \\ & \gamma_{12} & \end{bmatrix} \tag{2.19}$$

Consequently, the stress-generating strains are obtained by subtraction of the thermal- and moisture-induced strains from the total strains. The thermal- and moisture-induced strains are often approximated as linear functions of the changes in temperature and moisture concentration,

$$\begin{bmatrix} \varepsilon_1^T \\ \varepsilon_2^T \end{bmatrix} = \Delta T \begin{bmatrix} \alpha_1 \\ \alpha_2 \end{bmatrix} \tag{2.20}$$

$$\begin{bmatrix} \varepsilon_1^M \\ \varepsilon_2^M \end{bmatrix} = \Delta M \begin{bmatrix} \beta_1 \\ \beta_2 \end{bmatrix} \tag{2.21}$$

where ΔT and ΔM are the temperature change and moisture concentration change from the reference state.

The transformed thermal expansion coefficients ($\alpha_x, \alpha_y, \alpha_{xy}$) are obtained from those in the principal system using Equation (2.13). Note, however, that in the principal material coordinate system, there is no shear deformation induced [4], i.e., $\alpha_{16} = \beta_{16} = 0$,

$$\alpha_x = m^2\alpha_1 + n^2\alpha_2 \tag{2.22a}$$

$$\alpha_y = n^2\alpha_1 + m^2\alpha_2 \tag{2.22b}$$

$$\alpha_{xy} = 2mn(\alpha_1 - \alpha_2) \tag{2.22c}$$

The moisture expansion coefficients ($\beta_x, \beta_y, \beta_{xy}$) are obtained by replacing α with β in Equations (2.22).

The transformed constitutive relations for a lamina, when incorporating thermal- and moisture-induced strains, are

$$\begin{bmatrix} \varepsilon_x \\ \varepsilon_y \\ \gamma_{xy} \end{bmatrix} = \begin{bmatrix} \bar{S}_{11} & \bar{S}_{12} & \bar{S}_{16} \\ \bar{S}_{12} & \bar{S}_{22} & \bar{S}_{26} \\ \bar{S}_{16} & \bar{S}_{26} & \bar{S}_{66} \end{bmatrix} \begin{bmatrix} \sigma_x \\ \sigma_y \\ \tau_{xy} \end{bmatrix} + \begin{bmatrix} \varepsilon_x^T \\ \varepsilon_y^T \\ \gamma_{xy}^T \end{bmatrix} + \begin{bmatrix} \varepsilon_x^M \\ \varepsilon_y^M \\ \gamma_{xy}^M \end{bmatrix} \tag{2.23}$$

$$\begin{bmatrix} \sigma_x \\ \sigma_y \\ \tau_{xy} \end{bmatrix} = \begin{bmatrix} \bar{Q}_{11} & \bar{Q}_{12} & \bar{Q}_{16} \\ \bar{Q}_{12} & \bar{Q}_{22} & \bar{Q}_{26} \\ \bar{Q}_{16} & \bar{Q}_{26} & \bar{Q}_{66} \end{bmatrix} \begin{bmatrix} \varepsilon_x - \varepsilon_x^T - \varepsilon_x^M \\ \varepsilon_y - \varepsilon_y^T - \varepsilon_y^M \\ \gamma_{xy} - \gamma_{xy}^T - \gamma_{xy}^M \end{bmatrix} \tag{2.24}$$

2.2 Micromechanics

As schematically illustrated in Figure 2.5, micromechanics aims to describe the moduli and expansion coefficients of the lamina from properties of the fiber and matrix, the microstructure of the composite, and the volume fractions of the constituents. Sometimes, also the small transition region between bulk fiber and bulk matrix, i.e., interphase, is considered. Much fundamental work has been devoted to the study of the states of strain and stress in the constituents, and the formulation of appropriate averaging schemes to allow definition of macroscopic engineering constants. Most micromechanics analyses have focused on unidirectional continuous fiber composites, e.g. [9,10],

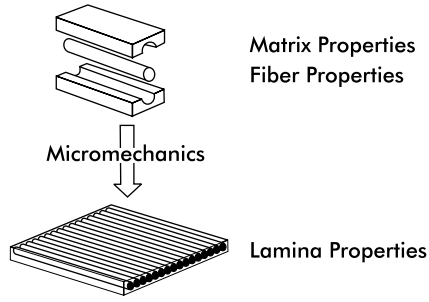

FIGURE 2.5
Role of micromechanics.

although properties of composites with woven fabric reinforcements can also be predicted with reasonable accuracy, see Reference [11].

The objective of this section is not to review the various micromechanics developments. The interested reader can find ample information in the above-referenced review articles. In this section, we will limit the presentation to some commonly used estimates of the stiffness constants, E_1, E_2, ν_{12}, ν_{21}, and G_{12}, and thermal expansion coefficients α_1 and α_2 required for describing the small strain response of a unidirectional lamina under mechanical and thermal loads (see Section 2.1). Such estimates may be useful for comparison to experimentally measured quantities.

2.2.1 Stiffness Properties of Unidirectional Composites

Although most matrices are isotropic, many fibers such as carbon and Kevlar (E.I. du Pont de Nemours and Company, Wilmington, DE,) have directional properties because of molecular or crystal plane orientation effects [4]. As a result, the axial stiffness of such fibers is much greater than the transverse stiffness. The thermal expansion coefficients along and transverse to the fiber axis also are quite different [4]. It is common to assume cylindrical orthotropy for fibers with axisymmetric microstructure. The stiffness constants required for plane stress analysis of a composite with such fibers are E_L, E_T, ν_{LT}, and G_{LT}, where L and T denote the longitudinal and transverse directions of a fiber. The corresponding thermal expansion coefficients are α_L and α_T.

The mechanics of materials approach reviewed in Reference [10] yields

$$E_1 = E_{Lf}V_f + E_mV_m \tag{2.25a}$$

$$E_2 = \frac{E_{Tf}E_m}{E_{Tf}V_m + E_mV_f} \tag{2.25b}$$

$$\nu_{12} = \nu_{LTf}V_f + \nu_mV_m \tag{2.25c}$$

$$G_{12} = \frac{G_{LTf} G_m}{G_{LTf} V_m + G_m V_f} \tag{2.25d}$$

where subscripts f and m represent fiber and matrix, respectively, and the symbol V represents volume fraction. Note that once E_1, E_2, and ν_{12} are calculated from Equations (2.25a), ν_{21} is obtained from Equation (2.8). Equations (2.25a) and (2.25c) provide good estimates of E_1 and ν_{12}. Equations (2.25b) and (2.25d), however, substantially underestimate E_2 and G_{12} [10]. More realistic estimates of E_2 and G_{12} are provided in References [10,12].

Simple, yet reasonable estimates of E_2 and G_{12} may also be obtained from the Halpin-Tsai equations [13],

$$P = \frac{P_m (1 + \xi \chi V_f)}{1 - \chi V_f} \tag{2.26a}$$

$$\chi = \frac{P_f - P_m}{P_f + \xi P_m} \tag{2.26b}$$

where P is the property of interest (E_2 or G_{12}) and P_f and P_m are the corresponding fiber and matrix properties, respectively. The parameter ξ is called the reinforcement efficiency; $\xi(E_2) = 2$ and $\xi(G_{12}) = 1$, for circular fibers.

2.2.2 Expansion Coefficients

Thermal expansion (and moisture swelling) coefficients can be defined by considering a composite subjected to a uniform increase in temperature (or moisture content) (Figure 2.4).

The thermal expansion coefficients, α_1 and α_2, of a unidirectional composite consisting of cylindrically or transversely orthotropic fibers in an isotropic matrix determined using the mechanics of materials approach [10] are

$$\alpha_1 = \frac{\alpha_{Lf} E_{Lf} V_f + \alpha_m E_m V_m}{E_{Lf} V_f + E_m V_m} \tag{2.27a}$$

$$\alpha_2 = \alpha_{Tf} V_f + \alpha_m V_m \tag{2.27b}$$

Predictions of α_1 using Equation (2.27a) are accurate [10], whereas Equation (2.27b) underestimates the actual value of α_2. An expression derived by Hyer and Waas [10] provides a more accurate prediction of α_2:

$$\alpha_2 = \alpha_{Tf} V_f + \alpha_m V_m + \frac{(E_{Lf} \nu_m + E_m \nu_{LTf})}{E_{Lf} V_f + E_m V_m} (\alpha_m - \alpha_{Lf}) V_f V_m \tag{2.28}$$

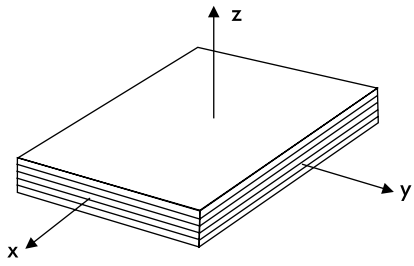

FIGURE 2.6
Laminate coordinate system.

2.3 Laminated Plate Theory

Structures fabricated from composite materials rarely utilize a single composite lamina because this unit is thin and anisotropic. To achieve a thicker cross section and more balanced properties, plies of prepreg or fiber mats are stacked in specified directions. Such a structure is called a laminate (Figure 2.6). Most analyses of laminated structures are limited to flat panels (see, e.g., References [1,2]). Extension to curved laminated shell structures may be found in References [5,14,15].

In this section, attention will be limited to a flat laminated plate under in-plane and bending loads. The classical theory of such plates is based on the assumption that a line originally straight and perpendicular to the middle surface remains straight and normal to the middle surface, and that the length of the line remains unchanged during deformation of the plate [1–6]. These assumptions lead to the vanishing of the out-of-plane shear and extensional strains:

$$\gamma_{xz} = \gamma_{yz} = \varepsilon_z = 0 \tag{2.29}$$

where the laminate coordinate system (x,y,z) is indicated in Figure 2.6. Consequently, the laminate strains are reduced to ε_x, ε_y, and γ_{xy}. The assumption that the cross sections undergo only stretching and rotation leads to the following strain distribution [1–6]:

$$\begin{bmatrix} \varepsilon_x \\ \varepsilon_y \\ \gamma_{xy} \end{bmatrix} = \begin{bmatrix} \varepsilon_x^0 \\ \varepsilon_y^0 \\ \gamma_{xy}^0 \end{bmatrix} + z \begin{bmatrix} \kappa_x \\ \kappa_y \\ \kappa_{xy} \end{bmatrix} \tag{2.30}$$

where $\left[\varepsilon_x^0, \varepsilon_y^0, \gamma_{xy}^0\right]$ and $\left[\kappa_x, \kappa_y, \kappa_{xy}\right]$ are the midplane strains and curvatures, respectively, and z is the distance from the midplane.

Force and moment resultants, $[N_x, N_y, N_{xy}]$ and $[M_x, M_y, M_{xy}]$, respectively, are obtained by integration of the stresses in each layer over the laminate thickness, h,

$$\begin{bmatrix} N_x \\ N_y \\ N_{xy} \end{bmatrix} = \int_{-h/2}^{h/2} \begin{bmatrix} \sigma_x \\ \sigma_y \\ \tau_{xy} \end{bmatrix}_k dz \tag{2.31}$$

$$\begin{bmatrix} M_x \\ M_y \\ M_{xy} \end{bmatrix} = \int_{-h/2}^{h/2} \begin{bmatrix} \sigma_x \\ \sigma_y \\ \tau_{xy} \end{bmatrix}_k zdz \tag{2.32}$$

where the subscript k represents the k^{th} lamina in the laminate. Combination of Equations (2.24) with (2.30–2.32) leads to the following constitutive relationships among forces and moments and midplane strains and curvatures:

$$\begin{bmatrix} N_x + N_x^T + N_x^M \\ N_y + N_y^T + N_y^M \\ N_{xy} + N_{xy}^T + N_{xy}^M \end{bmatrix} = \begin{bmatrix} A_{11} & A_{12} & A_{16} \\ A_{12} & A_{22} & A_{26} \\ A_{16} & A_{26} & A_{66} \end{bmatrix} \begin{bmatrix} \varepsilon_x^0 \\ \varepsilon_y^0 \\ \gamma_{xy}^0 \end{bmatrix} + \begin{bmatrix} B_{11} & B_{12} & B_{16} \\ B_{12} & B_{22} & B_{26} \\ B_{16} & B_{26} & B_{66} \end{bmatrix} \begin{bmatrix} \kappa_x \\ \kappa_y \\ \kappa_{xy} \end{bmatrix} \tag{2.33}$$

$$\begin{bmatrix} M_x + M_x^T + M_x^M \\ M_y + M_y^T + M_y^M \\ M_{xy} + M_{xy}^T + M_{xy}^M \end{bmatrix} = \begin{bmatrix} B_{11} & B_{12} & B_{16} \\ B_{12} & B_{22} & B_{26} \\ B_{16} & B_{26} & B_{66} \end{bmatrix} \begin{bmatrix} \varepsilon_x^0 \\ \varepsilon_y^0 \\ \gamma_{xy}^0 \end{bmatrix} + \begin{bmatrix} D_{11} & D_{12} & D_{16} \\ D_{12} & D_{22} & D_{26} \\ D_{16} & D_{26} & D_{66} \end{bmatrix} \begin{bmatrix} \kappa_x \\ \kappa_y \\ \kappa_{xy} \end{bmatrix} \tag{2.34}$$

where the A_{ij}, B_{ij}, and D_{ij} are called extensional stiffnesses, coupling stiffnesses, and bending stiffnesses, respectively [1–6], given by

$$A_{ij} = \sum_{k=1}^{N} \left(\overline{Q}_{ij}\right)_k \left(z_k - z_{k-1}\right) \tag{2.35a}$$

$$B_{ij} = \frac{1}{2} \sum_{k=1}^{N} \left(\overline{Q}_{ij}\right)_k \left(z_k^2 - z_{k-1}^2\right) \tag{2.35b}$$

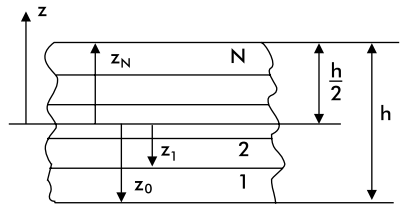

FIGURE 2.7
Definition of ply coordinates, z_k.

$$D_{ij} = \frac{1}{3}\sum_{k=1}^{N}\left(\overline{Q}_{ij}\right)_k\left(z_k^3 - z_{k-1}^3\right) \tag{2.35c}$$

The ply coordinates z_k, (k = 1, 2…N), where N is the number of plies in the laminate, are defined in Figure 2.7 and may be calculated from the following recursion formula:

$$z_0 = -h/2 \qquad k = 0 \tag{2.36a}$$

$$z_k = z_{k-1} + h_k \qquad k = 1, 2, \ldots, N \tag{2.36b}$$

in which h_k is the ply thickness of the kth ply.

For the steady-state condition considered, the temperature change is uniform throughout the laminate, and the thermal force resultants are determined from

$$\begin{bmatrix} N_x^T \\ N_y^T \\ N_{xy}^T \end{bmatrix} = \sum_{k=1}^{N}\begin{bmatrix} \overline{Q}_{11} & \overline{Q}_{12} & \overline{Q}_{16} \\ \overline{Q}_{12} & \overline{Q}_{22} & \overline{Q}_{26} \\ \overline{Q}_{16} & \overline{Q}_{26} & \overline{Q}_{66} \end{bmatrix}_k \begin{bmatrix} \alpha_x \\ \alpha_y \\ \alpha_{xy} \end{bmatrix}_k (z_k - z_{k-1})\Delta T \tag{2.37}$$

The moisture-induced force resultants $[N_x^M, N_y^M, N_{xy}^M]$ are obtained in the same manner as the thermal force resultants, but by replacing $[\alpha_x, \alpha_y, \alpha_{xy}]$ with $[\beta_x, \beta_y, \beta_{xy}]$, and ΔT with ΔM in Equation (2.37).

The thermal moment resultants $[M_x^T, M_y^T, M_{xy}^T]$ are determined from

$$\begin{bmatrix} M_x^T \\ M_y^T \\ M_{xy}^T \end{bmatrix} = \frac{1}{2}\sum_{k=1}^{N}\begin{bmatrix} \overline{Q}_{11} & \overline{Q}_{12} & \overline{Q}_{16} \\ \overline{Q}_{12} & \overline{Q}_{22} & \overline{Q}_{26} \\ \overline{Q}_{16} & \overline{Q}_{26} & \overline{Q}_{66} \end{bmatrix}_k \begin{bmatrix} \alpha_x \\ \alpha_y \\ \alpha_{xy} \end{bmatrix}_k (z_k^2 - z_{k-1}^2)\Delta T \tag{2.38}$$

The moisture-induced moment resultants $[M_x^M, M_y^M, M_{xy}^M]$ are obtained by replacing the α values with β values and ΔT with ΔM in Equations (2.38).

Most commonly, only the steady-state temperature and moisture concentration in the composite is of interest (ΔT and ΔC are constants). However, in a transient situation, the transfer of heat by conduction [16], or moisture diffusion [17,18] has to be considered. Pipes et al. [19] examined laminated plates subject to transient conditions. For laminates with the plies consisting of different materials, the moisture concentration may vary through the thickness in a stepwise manner. At steady-state this is incorporated into the analysis by letting $\Delta M = (\Delta M)_k$, [20].

Equations (2.33) and (2.34) may conveniently be written as

$$\begin{bmatrix} N \\ M \end{bmatrix} = \begin{bmatrix} A & B \\ B & D \end{bmatrix} \begin{bmatrix} \varepsilon^0 \\ \kappa \end{bmatrix} \tag{2.39}$$

where [N] and [M] represent the left-hand side of Equations (2.33) and (2.34), i.e., the sum of mechanical and hygrothermal forces and moments, respectively.

Equations (2.39) represent the stiffness form of the laminate constitutive equations. Sometimes it is more convenient to express the midplane strains and curvatures as a function of the forces and moments. This represents the compliance form of the laminate constitutive equations, which is obtained by inversion of Equations (2.39),

$$\begin{bmatrix} \varepsilon^0 \\ \kappa \end{bmatrix} = \begin{bmatrix} A' & B' \\ C' & D' \end{bmatrix} \begin{bmatrix} N \\ M \end{bmatrix} \tag{2.40}$$

Expressions for the matrices [A′], [B′], [C′], and [D′] are given in Appendix A.

2.4 St. Venant's Principle and End Effects in Composites

In the testing and evaluation of any material, it is generally assumed that load introduction effects are confined to a region close to the grips or loading points, and a uniform state of stress and strain exists within the test section. The justification for such a simplification is usually based on the St. Venant principle, which states that the difference between the stresses caused by statically equivalent load systems is insignificant at distances greater than the largest dimension of the area over which the loads are acting [21]. This estimate, however, is based on isotropic material properties. For anisotropic composite materials, Horgan et al. [22–25] showed that the application of St. Venant's principle for plane elasticity problems involving anisotropic materials is not justified in general. For the particular problem of a rectangular strip made of

highly anisotropic material and loaded at the ends, it was demonstrated that the stress approached the uniform St. Venant solution much more slowly than the corresponding solution for an isotropic material [23].

The size of the region where end effects influence the stresses in a rectangular strip loaded with tractions at the ends is given by [23]

$$\lambda \approx \frac{b}{2\pi}\left(E_1/G_{12}\right)^{1/2} \tag{2.41}$$

where b is the maximum dimension of the cross section, and E_1 and G_{12} are the longitudinal elastic and shear moduli, respectively.

In this equation λ is defined as the distance over which the self-equilibrated stress decays to 1/e of its value at the end. When the ratio E_1/G_{12} is large, the decay length is large and end effects are transferred a considerable distance along the gage section. Testing of highly anisotropic materials thus requires special consideration of load introduction effects. Arridge et al. [26], for example, found that a very long specimen with an aspect ratio ranging from 80 to 100 was needed to avoid the influence of clamping effects in tension testing of highly anisotropic, drawn polyethylene film. Several other cases are reviewed in Reference [25].

2.5 Lamina Strength Analysis

When any material is considered for a structure, an important task for the structural engineer is to assess the load-carrying ability of the particular material/structure combination. Prediction of the strength of composite materials has been an active area of research since the early work of Tsai [27]. Many failure theories have been suggested, although no universally accepted failure criterion exists [28]. As pointed out by Hyer [4], however, no single criterion could be expected to accurately predict failure of all composite materials under all loading conditions. Popular strength criteria are maximum stress, maximum strain, and Tsai-Wu criteria (see References [1–6,28]). These criteria are phenomenological in the sense that they do not rely on physical modeling of the failure process. The reason for their popularity is that they are based on failure tests on simple specimens in tension, compression, and shear (Chapters 5–7) and are able to predict load levels required to fail more complicated structures under combined stress loading.

In the following presentation, failure of the lamina will first be examined and then failure of the laminate will be briefly considered. It is assumed that the lamina, being unidirectional or a woven fabric ply, can be treated as a homogeneous orthotropic ply with known, measured strengths in the principal material directions. Furthermore, the shear strength in the plane of the

TABLE 2.1

Basic Strengths of Orthotropic Plies for Plane Stress

Direction/Plane	Active Stress	Strength	Ultimate Strain
1	σ_1	X_1^T, X_1^C	e_1^T, e_1^C
2	σ_2	X_2^T, X_2^C	e_2^T, e_2^C
1,2	τ_{12}	S_6	e_6

Note: All strengths and ultimate strains are defined by their magnitudes.

fibers is independent of the sign of the shear stress. The presentation is limited to plane stress in the plane of the fibers. Table 2.1 lists the five independent failure stresses and strains corresponding to plane stress.

Notice here that superscripts T and C denote tension and compression, respectively, and that strengths and ultimate strains are defined as positive, i.e., the symbols indicate their magnitudes. For example, a composite ply loaded in pure negative shear ($\tau_{12} < 0$) would fail at a shear stress $\tau_{12} = -S_6$ and shear strain $\gamma_{12} = -e_6$.

2.5.1 Maximum Stress Failure Criterion

The maximum stress failure criterion assumes that failure occurs when any one of the in-plane stresses σ_1, σ_2, or τ_{12} attains its limiting value independent of the other components of stress. If the magnitudes of the stress components are less than their values at failure, failure does not occur, and the element or structure is considered safe. For determining the failure load, any of the following equalities must be satisfied at the point when failure occurs:

$$\sigma_1 = X_1^T \tag{2.42a}$$

$$\sigma_1 = -X_1^C \tag{2.42b}$$

$$\sigma_2 = X_2^T \tag{2.42c}$$

$$\sigma_2 = -X_2^C \tag{2.42d}$$

$$\tau_{12} = S_6 \tag{2.42e}$$

$$\tau_{12} = -S_6 \tag{2.42f}$$

For unidirectional and fabric composites, Equations (2.42a and b) indicate failure of fibers at quite high magnitudes of stress, whereas Equations (2.4c–f) indicate matrix or fiber–matrix interface dominated failures at much lower

magnitudes of stress for unidirectional composites. For fabric composites, however, Equations (2.42c and d) indicate failure of the fibers oriented along the 2-direction.

2.5.2 Maximum Strain Failure Criterion

The maximum strain criterion assumes that failure of any principal plane of the lamina occurs when any in-plane strain reaches its ultimate value in uniaxial tension, compression, or pure shear. Failure should occur when any of the following equalities are satisfied (Table 2.1):

$$\varepsilon_1 = e_1^T \tag{2.43a}$$

$$\varepsilon_1 = -e_1^C \tag{2.43b}$$

$$\varepsilon_2 = e_2^T \tag{2.43c}$$

$$\varepsilon_2 = -e_2^C \tag{2.43d}$$

$$\gamma_{12} = e_6 \tag{2.43e}$$

$$\gamma_{12} = -e_6 \tag{2.43f}$$

In these expressions, the symbol e represents the magnitude of the ultimate strain. If any of the above conditions become satisfied, failure is assumed to occur by the same mechanism leading to failure in uniaxial loading or pure shear loading. Similar to the maximum stress criterion, the maximum strain criterion has the ability of predicting the failure mode.

2.5.3 Tsai-Wu Failure Criterion

Tsai and Wu [29] proposed a second-order tensor polynomial failure criterion for prediction of biaxial strength, which takes the following form for plane stress:

$$F_1\sigma_1 + F_2\sigma_2 + F_{11}\sigma_1^2 + F_{22}\sigma_2^2 + F_{66}\tau_{12}^2 + 2F_{12}\sigma_1\sigma_2 = 1 \tag{2.44}$$

Failure under combined stress is assumed to occur when the left-hand side of Equation (2.44) is equal to or greater than one. All of the parameters of the Tsai-Wu criterion, except F_{12}, can be expressed in terms of the basic strengths (Table 2.1).

$$F_1 = 1/X_1^T - 1/X_1^C \qquad F_{11} = 1/\left(X_1^T X_1^C\right)$$
$$F_2 = 1/X_2^T - 1/X_2^C \qquad F_{22} = 1/\left(X_2^T X_2^C\right) \tag{2.45}$$
$$F_{66} = 1/S_6^2$$

F_{12} is a strength interaction parameter that has to be determined from a biaxial experiment. Such experiments are, unfortunately, very expensive and difficult to properly conduct. As an alternative, Tsai and Hahn [30] suggested that F_{12} be estimated from the following relationship:

$$F_{12} = -\frac{1}{2}\sqrt{F_{11}F_{22}} \tag{2.46}$$

The Tsai-Wu criterion has found widespread applicability in the composite industry because of its versatility and that it provides quite accurate predictions of strength. It does not, however, predict the mode of failure.

2.6 Laminate Strength Analysis

Analysis of failure and strength of laminated composites is quite different from the analysis of strength of a single ply. Failure of laminates commonly involves delamination, i.e., separation of the plies, which will be discussed in Chapter 14. This failure mode is commonly influenced by the three-dimensional state of stress that develops near free edges in laminated specimens [31]. Furthermore, multidirectional composite laminates are commonly processed at elevated temperatures and the mismatch in thermal expansion between the plies leads to residual stresses in the plies upon cooling [32–34]. Exposure of the laminate to moisture will also influence the state of residual stress in the laminate [18,35].

A common failure mode in laminates containing unidirectional plies is matrix cracking, which is failure of the matrix and fiber–matrix interface in a plane perpendicular to the fiber direction (Figure 2.8). Such a failure is called first-ply failure and occurs because of the presence of a weak plane transverse to the fiber axis in such composites. In fabric composites, no such weak planes exist, and failure initiates locally in fiber tows and matrix pockets before ultimate failure occurs [36]. At any instant, local failures tend to arrest by constraint of adjacent layers or tows in the laminate before the occurrence of catastrophic failure of the laminate. Wang and Crossman et al. [37–39] and Flaggs and Kural [40] found a very large constraint effect in composite laminates with unidirectional plies. They examined matrix cracking in a set of

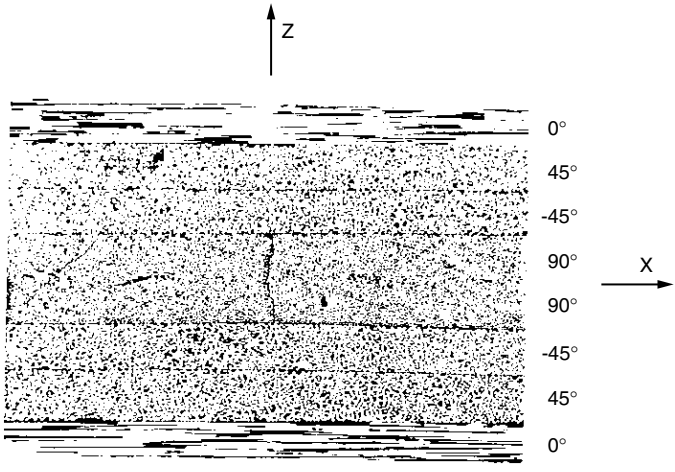

FIGURE 2.8
Matrix crack of a unidirectional ply in a laminate (first-ply failure).

laminates containing unidirectional 90° plies bonded together and found that the *in situ* strength depends strongly on the number of plies of the same orientation bonded together, and on the adjacent ply orientations. Consequently, there are a host of mechanisms influencing failure of laminates, and as a result, accurate failure prediction is associated with severe difficulties.

Various methods to predict ply failures and ultimate failure of composite laminates are reviewed by Sun [28]. A common method in laminate failure analysis is to determine the stresses and strains in the laminate using laminated plate theory (Section 2.3), and then examine the loads and strains corresponding to the occurrence of first-ply failure as predicted by the failure criterion selected. The ply failure mode is then identified. Swanson and Trask [41] and Swanson and Qian [42] performed biaxial tension–tension and tension–compression testing on several carbon/epoxy laminate cylinders made from unidirectional plies. Ply failures were identified using strength criteria mentioned in Section 2.5. Final failure of the cylinders was predicted by using a ply property reduction method (ply-by-ply discount method) where failed plies are identified and the transverse and shear moduli (E_2 and G_{12}) of the failed plies are assigned numbers very close to zero. The laminate with reduced stiffness is then again analyzed for stresses and strains [28]. Comparison of the predictions with measured ultimate failure data of the cylinders revealed good agreement for all criteria. It was concluded that the maximum stress and maximum strain criteria are quite insensitive to variations in the ply transverse failure strengths (X_2^T and S_6). This is an advantage because, as discussed, these strengths are very difficult to determine *in situ*. Hence, the failure criteria that do not demand accurate transverse ply failure strengths were concluded to be the most pertinent for failure prediction. For further reading, see References [1–6] and [28].

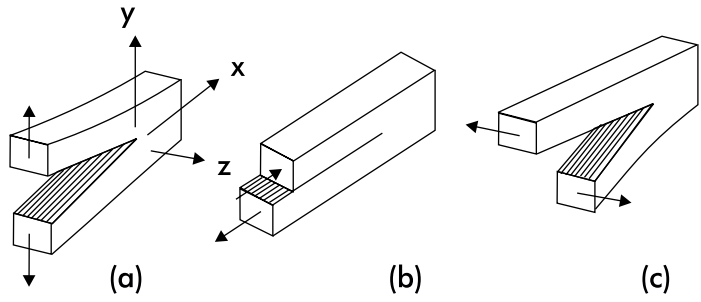

FIGURE 2.9
Modes of crack surface displacements. (a) Mode I (opening), (b) Mode II (sliding), and (c) Mode III (tearing).

2.7 Fracture Mechanics Concepts

The influence of defects and cracks on the strength of a material or structure is the subject of fracture mechanics. The object of fracture mechanics analysis is the prediction of the onset of crack growth for a body containing a flaw of a given size. To calculate the critical load for a cracked composite, it has generally been assumed that the size of the plastic zone at the crack tip is small compared to the crack length. Linear elastic fracture mechanics has been found useful for certain types of cracks in composites, i.e., interlaminar cracks [43] or matrix cracks in a unidirectional composite [37,44].

The equilibrium of an existing crack may be judged from the intensity of elastic stress around the crack tip. Solutions of the elastic stress field in isotropic [45] and orthotropic [46] materials show that stress singularities associated with in-plane cracks are of the $r^{-1/2}$ type, where r is the distance from the crack tip. Stress intensity factors may be determined for crack problems where the crack plane is in any of the planes of orthotropic material symmetry. It is possible to partition the crack tip loading into the three basic modes of crack surface displacement shown in Figure 2.9. Mode I refers to opening of the crack surfaces, Mode II refers to sliding, and Mode III refers to tearing.

It has, however, become common practice to investigate interlaminar cracks using the strain energy release rate, G. This quantity is based on energy considerations and is mathematically well defined and measurable in experiments. The energy approach, which stems from the original Griffith treatment [47], is based on a thermodynamic criterion for fracture by considering the energy available for crack growth of the system on one hand, and the surface energy required to extend an existing crack on the other hand. An elastic potential for a cracked body may be defined as

$$H = W - U \tag{2.47}$$

where W is the work supplied by the movement of the external forces, and U is the elastic strain energy stored in the body. If G_c is the work required to create a unit crack area, it is possible to formulate a criterion for crack growth,

$$\delta H \geq G_c \delta A \tag{2.48}$$

where δA is the increase in crack area.

A critical condition occurs when the net energy supplied just balances the energy required to grow the crack; i.e.,

$$\delta H = G_c \delta A \tag{2.49}$$

Equilibrium becomes unstable when the net energy supplied exceeds the required crack growth energy,

$$\delta H > G_c \delta A \tag{2.50}$$

The strain energy release rate, G, is defined as

$$G = \frac{\partial H}{\partial A} \tag{2.51}$$

In terms of G, the fracture criterion may thus be formulated as

$$G \geq G_c \tag{2.52}$$

This concept will be illustrated for a linear elastic body containing a crack of original length, a. Figure 2.10 shows the load, P, vs. displacement, u, for the cracked body where crack growth is assumed to occur either at constant load (fixed load) or at constant displacement (fixed grip).

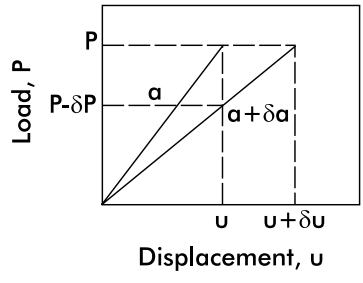

FIGURE 2.10
Load-displacement behavior for a cracked body at crack lengths a and a + δa.

For the *fixed-load* case,

$$\delta U = \frac{P\delta u}{2} \tag{2.53a}$$

$$\delta W = P\delta u \tag{2.53b}$$

Equation (2.47) gives

$$\delta H = P\delta u - P\delta u/2 = P\delta u/2 \tag{2.54}$$

and Equation (2.51) gives

$$G = \frac{P}{2}\frac{\partial u}{\partial A} \tag{2.55}$$

For the *fixed-grip* case, the work term in Equation (2.47) vanishes and

$$\delta U = \frac{u\delta P}{2} \tag{2.56}$$

Note that δP is negative because of the loss in stiffness followed by crack extension, and G is

$$G = -\frac{u}{2}\frac{\partial P}{\partial A} \tag{2.57}$$

For a linear elastic body, the relationship between load and displacement may be expressed as

$$u = CP \tag{2.58}$$

where C is the compliance of the specimen. Substitution into Equation (2.55) (fixed load) gives

$$G = \frac{P^2}{2}\frac{\partial C}{\partial A} \tag{2.59}$$

For the fixed-grip case, substitution of $P = u/C$ into Equation (2.57) gives

$$G = \frac{u^2}{2C^2}\frac{\partial C}{\partial A} = \frac{P^2}{2}\frac{\partial C}{\partial A} \tag{2.60}$$

Consequently, both fixed-load and fixed-grip conditions give the same expression. This expression is convenient for the experimental determination of G and will be employed in Chapter 14 for derivation of expressions for G for various delamination fracture specimens.

For a crack in a principal material plane, it is possible to decompose G into components associated with the three basic modes of crack extension illustrated in Figure 2.9:

$$G = G_I + G_{II} + G_{III} \tag{2.61}$$

Theoretically, the mode separation is based on Irwin's contention that if the crack extends by a small amount, Δa, the energy absorbed in the process is equal to the work required to close the crack to its original length [48]. For a polar coordinate system with the origin at the extended crack tip (Figure 2.9), the various contributions to the total energy release rate are

$$G_I = \lim_{\Delta a \to 0} \frac{1}{2\Delta a} \int_0^{\Delta a} \sigma_y(\Delta a - r)\overline{v}(r,\pi)dr \tag{2.62a}$$

$$G_{II} = \lim_{\Delta a \to 0} \frac{1}{2\Delta a} \int_0^{\Delta a} \tau_{xy}(\Delta a - r)\overline{u}(r,\pi)dr \tag{2.62b}$$

$$G_{III} = \lim_{\Delta a \to 0} \frac{1}{2\Delta a} \int_0^{\Delta a} \tau_{yz}(\Delta a - r)\overline{w}(r,\pi)dr \tag{2.62c}$$

where r is the radial distance from the crack tip, σ_y, τ_{xy} and τ_{yz} are the normal and shear stresses near the crack tip; and $\overline{v}, \overline{u}$, and $\overline{w}$ are the relative opening and sliding displacements between points on the crack faces, respectively. These expressions form the basis for the virtual crack closure (VCC) method for separation of the fracture modes using finite element solutions of crack problems [49].

2.8 Strength of Composite Laminates Containing Holes

Structures made from composite laminates containing cutouts or penetrations such as fastener holes (notches) offer a special challenge to the designer because of the stress concentration associated with the geometric discontinuity. In laminates containing notches, a complex fiber-bridging zone develops near the notch tip [50,51]. On the microscopic level, the damage appears in the

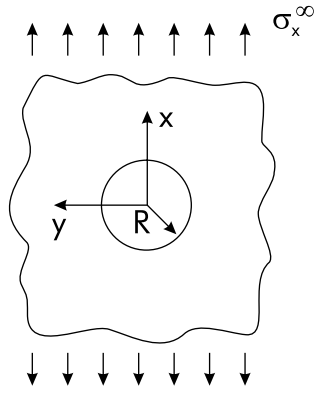

FIGURE 2.11
Infinite plate containing a circular hole under remote uniform tension.

form of fiber pullout, matrix microcracking, and fiber–matrix interfacial failure. The type of damage and its growth depends strongly on the laminate stacking sequence, type of resin, and the fiber. As a consequence of the damaged material, the assumptions of a small process zone and self-similar growth of a single crack, inherent in linear elastic fracture mechanics, break down. In experimental studies on notched laminates under tension or compression loads, the strength is substantially reduced compared to the strength of the unnotched specimen [51,52].

Because of the complexity of the fracture process for notched composite laminates, the methods developed for prediction of strength are semiempirical. Awerbuch and Madhukar [52] review strength models for laminates containing cracks or holes loaded in tension. In this text, only the technically important case of a laminate containing a circular hole will be considered.

A conservative estimate of the strength reduction is based on the stress concentration factor at the hole edge for a composite laminate containing a circular hole,

$$\frac{\sigma_N}{\sigma_0} = \frac{1}{K} \tag{2.63}$$

where σ_N and σ_0 are the notched and unnotched ultimate strengths of the laminate, and K is the stress concentration factor. The stress distribution can be obtained in closed form only for infinite, homogeneous, orthotropic plates containing an open hole [53]. The stress concentration factor, K_∞, for an infinite plate containing a circular hole (Figure 2.11) is given in terms of the effective orthotropic engineering constants of the plate [53],

$$K_\infty = 1 + \sqrt{2\left(\sqrt{E_x / E_y} - \nu_{xy} + E_x / (2G_{xy})\right)} \tag{2.64}$$

where x and y are coordinates along and transverse to the loading direction (Figure 2.11). The stress concentration factor for finite-width plates containing holes is larger than K_∞ [54,55]. Plates where the width and length exceed about six hole diameters, however, may be considered as infinite, and Equation (2.64) holds to a good approximation.

It can be easily verified from Equation (2.64) that the stress concentration factor for an isotropic material is 3. For highly anisotropic composites, the stress concentration factor is much greater (up to 9 for unidirectional carbon/epoxy).

References

1. I.M. Daniel and O. Ishai, *Engineering Mechanics of Composite Materials*, Oxford University Press, New York, 1994.
2. R.F. Gibson, *Principles of Composite Materials Mechanics,* McGraw-Hill, New York, 1994.
3. J.N. Reddy, *Mechanics of Laminated Composite Materials — Theory and Analysis*, CRC Press, Boca Raton, FL, 1997.
4. M.W. Hyer, *Stress Analysis of Fiber-Reinforced Composite Materials*, WCB/McGraw-Hill, Boston, 1998.
5. C.T. Herakovich, *Mechanics of Fibrous Composites*, John Wiley & Sons, New York, 1998.
6. R.M. Jones, *Mechanics of Composite Materials*, 2nd ed., Taylor & Francis, Philadelphia, 1999.
7. Z. Hashin, Analysis of composite materials — a survey, *J. Appl. Mech.*, 50, 481–505, 1983.
8. J.C. Halpin and N.J. Pagano, Consequences of environmentally induced dilatation in solids, *Recent Adv. Eng. Sci.*, 5, 33–46, 1970.
9. R.M. Christensen, *Mechanics of Composite Materials*, John Wiley & Sons, New York, 1979.
10. M.Y. Hyer and A.M. Waas, Micromechanics of linear elastic continuous fiber composite, in *Comprehensive Composite Materials*, A. Kelly and C. Zweben, eds., Vol. 1, Elsevier, Oxford, 2000, pp. 345–375.
11. J.-H. Byun and T. –W. Chou, Mechanics of textile composites, in *Comprehensive Composite Materials*, A. Kelly and C. Zweben, eds., Vol. 1, Elsevier, Oxford, 2000, pp. 719–761.
12. B.W. Rosen and Z. Hashin, Analysis of material properties, in *Engineered Materials Handbook*, Vol. 1, Composites, T.J. Reinhart, tech. chairman, ASM International, Metals Park, OH, 1987, pp. 185–205.
13. J.C. Halpin and J.L. Kardos, The Halpin-Tsai equations: a review, *Polym. Eng. Sci.*, 16, 344–352, 1976.
14. M.W. Hyer, Laminated plate and shell theory, in *Comprehensive Composite Materials*, A. Kelly and C. Zweben, eds., Vol. 1, Elsevier, Oxford, 2000, pp. 479–510.
15. J.R. Vinson and R.L. Sierakowsky, *The Behavior of Structures Composed of Composites Materials*, 2nd ed., Kluwer, Dordrecht, 2002.
16. M.N. Ozisik, *Heat Conduction*, John Wiley & Sons, New York, 1980.

17. W. Jost, *Diffusion*, 3rd ed., Academic Press, New York, 1960.
18. G.S. Springer, ed., *Environmental Effects on Composite Materials*, Technomic, Lancaster, PA, 1981.
19. R.B. Pipes, J.R. Vinson, and T.W. Chou, On the hygrothermal response of laminated composite systems, *J. Compos. Mater.*, 10, 129–148, 1976.
20. L.A. Carlsson, Out-of-plane hygroinstability of multi-ply paperboard, *Fibre Sci. Technol.*, 14, 201–212, 1981.
21. S.P. Timoshenko and J.N. Goodier, *Theory of Elasticity*, 3rd ed., McGraw-Hill, New York, 1970.
22. C.O. Horgan, Some remarks on Saint-Venant's principle for transversely isotropic composites, *J. Elasticity*, 2(4), 335–339, 1972.
23. I. Choi and C.O. Horgan, Saint-Venant's principle and end effects in anisotropic elasticity, *J. Appl. Mech.*, 44, 424–430, 1977.
24. C.O. Horgan, Saint-Venant end effects in composites, *J. Compos. Mater.*, 16, 411–422, 1982.
25. C.O. Horgan and L.A. Carlsson, Saint-Venant end effects for anisotropic materials, in *Comprehensive Composite Materials*, A. Kelly and C. Zweben, eds., Vol. 5, Elsevier, Oxford, 2000, pp. 5–21.
26. R.G.C. Arridge, P.I. Barham, C.J. Farell, and A. Keller, The importance of end effects in the measurement of moduli of highly anisotropic materials, *J. Mater. Sci.*, 11, 788–790, 1976.
27. S.W. Tsai, Strength theories of filamentary structures, in *Fundamental Aspects of Fiber Reinforced Plastic Composites*, R.T. Schwartz and H.S. Schwartz, eds., John Wiley & Sons, New York, 1968, pp. 3–11.
28. C.T. Sun, Strength analysis of unidirectional composites and laminates, in *Comprehensive Composite Materials*, A. Kelly and C. Zweben, eds., Vol. 1, Elsevier, Oxford, 2000, pp. 641–666.
29. S.W. Tsai and E.M. Wu, A general theory of strength for anisotropic materials, *J. Compos. Mater.*, 5, 58–80, 1971.
30. S.W. Tsai and H.T. Hahn, *Introduction to Composite Materials*, Technomic, Lancaster, PA, 1980.
31. R.B. Pipes, B.E. Kaminski, and N.J. Pagano, Influence of the free-edge upon the strength of angle-ply laminates, *ASTM Spec. Tech. Publ.*, 521, 218–228, 1973.
32. H.T. Hahn and N.J. Pagano, Curing stresses in composite laminates, *J. Compos. Mater.*, 9, 91–106, 1975.
33. Y. Weitsman, Residual thermal stresses due to cool-down of epoxy-resin composites, *J. Appl. Mech.*, 46, 563–567, 1979.
34. G. Jeronimidis and A.T. Parkyn, Residual stresses in carbon fibre-thermoplastic matrix laminates, *J. Compos. Mater.*, 22, 401–415, 1988.
35. L. Carlsson, C. Eidefeldt, and T. Mohlin, Influence of sublaminate cracks on the tension fatigue behavior of a graphite/epoxy laminate, *ASTM Spec. Tech. Publ.*, 907, 361–382, 1986.
36. N. Alif and L.A. Carlsson, Failure mechanisms of woven carbon and glass composites, *ASTM Spec. Tech. Publ.*, 1285, 471–493, 1997.
37. A.S.D. Wang and F.W. Crossman, Initiation and growth of transverse cracks and edge delamination in composite laminates. Part 1. An energy method, *J. Compos. Mater. Suppl.* 14, 71–87, 1980.
38. F.W. Crossman, W.J. Warren, A.S.D. Wang, and G.E. Law, Jr., Initiation and growth of transverse cracks and edge delamination in composite laminates. Part 2. Experimental correlation, *J. Compos. Mater. Suppl.* 14, 88–108, 1980.

39. F.W. Crossman and A.S.D. Wang, The dependence of transverse cracking and delamination on ply thickness in graphite/epoxy laminates, *ASTM Spec. Tech. Publ.*, 775, 118–139, 1982.
40. D.L. Flaggs and M.H. Kural, Experimental determination of the in-situ transverse lamina strength in graphite/epoxy laminates, *J. Compos. Mater.*, 16, 103–115, 1982.
41. S.R. Swanson and B.C. Trask, Strength of quasi-isotropic laminates under off axis loading, *Compos. Sci. Technol.*, 34, 19–34, 1989.
42. S.R. Swanson and Y. Qian, Multiaxial characterization of T300/3900-2 carbon/epoxy composites, *Compos. Sci. Technol.*, 43, 197–203, 1992.
43. D.J. Wilkins, J.R. Eisenmann, R.A. Camin, W.S. Margolis, and R.A. Benson, Characterizing delamination growth in graphite-epoxy, *ASTM Spec. Tech. Publ.*, 775, 168–183, 1982.
44. E.M. Wu, Application of fracture mechanics to anisotropic plates, *J. Appl. Mech.*, 34, 967–974, 1967.
45. H.M. Westergaard, Bearing pressure and cracks, *J. Appl. Mech.*, 6, A49–A53, 1939.
46. G.C. Sih, P.C. Paris, and G.R. Irwin, On cracks in rectilinearly anisotropic bodies, *Int. J. Fract. Mech.*, 1(3), 189–203, 1965.
47. A.A. Griffith, The phenomena of rupture and flow in solids, *Phil. Trans. R. Soc.*, A221, 163–198, 1920.
48. G.R. Irwin, Fracture, in *Handbuch der Physik*, Vol. 6, S. Flügge, ed., Springer, Berlin, 1958, pp. 551–590.
49. E.F. Rybicki and M.F. Kanninen, A finite element calculation of stress intensity factors by a modified crack closure integral, *Eng. Fract. Mech.*, 9, 931–938, 1977.
50. J.F. Mandell, S.S. Wang, and F.J. McGarry, The extension of crack tip damage zones in fiber reinforced plastic laminates, *J. Compos. Mater.*, 9, 266–287, 1975.
51. C.G. Aronsson, Tensile Fracture of Composite Laminates with Holes and Cracks, Ph.D. dissertation, The Royal Institute of Technology, Stockholm, Sweden, 1984.
52. J. Awerbuch and M.S. Madhukar, Notched strength of composite laminates, *J. Reinf. Plast. Compos.*, 4, 3–159, 1985.
53. S.G. Lekhnitskii, *Anisotropic Plates*, Gordon and Breach, New York, 1968.
54. H.J. Konish and J.M. Whitney, Approximate stresses in an orthotropic plate containing a circular hole, *J. Compos. Mater.*, 9, 157–166, 1975.
55. J.W. Gillespie, Jr., and L.A. Carlsson, Influence of finite width on notched laminate strength predictions, *Compos. Sci. Technol.*, 32, 15–30, 1988.